On the sensitivity of heat transfer in the stagnation-point boundary layer to free-stream vorticity

By S. P. SUTERA, P. F. MAEDER AND J. KESTIN
Division of Engineering, Brown University, Providence, Rhode Island

(Received 10 August 1962 and in revised form 11 March 1963)

Experiments have given evidence of strong sensitivity of the stagnation-point heat transfer on cylinders to small changes in the intensity of free-stream turbulence. A similar effect on local heat-transfer rates to flat plates has been measured, but only when a favourable pressure gradient is present. In this work it is theorized that vorticity amplification by stretching is a possible, and perhaps the dominant, underlying mechanism responsible for this sensitivity. A mathematical model is presented for a steady, basically plane stagnation flow into which is steadily transported disturbed unidirectional vorticity having the only orientation susceptible to stretching. The resulting velocity and temperature fields in the stagnation-point boundary layer are analysed assuming the fluid to be incompressible and to have constant properties. By means of iterative procedures and electronic analogue computation an approximate solution to the full Navier–Stokes equations is achieved which indicates that amplification by stretching of vorticity of sufficiently large scale can occur. Such vorticity, present in the oncoming flow with a small intensity, can appear near the boundary layer with an amplified intensity and induce substantial three-dimensional effects therein. It is found that the thermal boundary layer is much more sensitive to the induced effects than the velocity boundary layer. Computations indicate that a certain amount of distributed vorticity in the oncoming flow causes the shear stress at the wall to increase by 5 %, while the heat transfer there is augmented by 26 % in a fluid with a Prandtl number of 0·74. Preliminary computations reveal that the sensitivity of the thermal boundary layer increases with Prandtl number.

1. Introduction

In the recent past considerable attention has been given to the problem of the influence of oscillations or turbulence on stable laminar boundary layers. The stimulus for the interest in this area is due largely to the considerable discrepancies evident in the results of certain experiments in forced convective heat transfer. From the beginning the interaction between turbulence or oscillations in the free stream and the boundary layers on solid surfaces was suspected as the cause of these discrepancies. An extensive discussion of the background of the subject can be found in a report by Kestin & Maeder (1957).

Numerous investigations, both theoretical and experimental, into the mechanism of the effect of free-stream fluctuations on heat transfer have been under-

taken. The measurements of Kestin & Maeder (1957), Kestin, Maeder & Sogin (1961), Kestin, Maeder & Wang (1961*a*; *b*), Giedt (1951), Sato & Sage (1958), and Short, Brown & Sage (1960) attest to the considerable influence of the effect in certain types of flow. For instance, it has been measured by Kestin, Maeder & Sogin (1961) that an increase in free-stream turbulence from 0·5 to 2·7 % will increase the heat transfer across a stagnation-point boundary layer by more than 40 % to a level nearly 80 % above the theoretical zero-turbulence prediction. Heretofore theoretical investigations into this problem have not succeeded in predicting influences of such large magnitudes.

Turbulent flow, in general, contains three-dimensional vorticity and is unsteady, since the vorticity is compelled to move with the fluid. Consequently, the mathematical formulation of such a flow must be exceedingly complex. It is understandable, therefore, that greatly simplified mathematical models were treated in the theoretical analyses of this problem. The oldest and possibly the simplest was that of a harmonically incompressible main stream containing no vorticity. This type of model was analysed by Schlichting (1932). (His calculation is very adequately described in the book by the same author, Schlichting 1960.) He considered small amplitude oscillations and found that a potential flow which fluctuates periodically in time gives rise to a steady, secondary 'streaming' motion both near and far from the wall. Schlichting, however, made no heat-transfer calculations. Lighthill (1954) studied the response of the boundary layer adjacent to a fixed cylindrical body when the external flow velocity has a steady direction but a magnitude which fluctuates harmonically about a steady mean. The approximate solution which he gave was correct only to first order in the amplitude of the fluctuations, and consequently did not predict secondary flow, a second-order effect.

Subsequent theoretical efforts dealt with main streams which varied arbitrarily but continuously with time, and also with the special situation of a steady main stream with superimposed harmonic oscillations. Moore (1951) considered both types of flow past an insulated flat plate and defined the circumstances under which the boundary-layer flow could be regarded as quasi-steady. This work was extended by Ostrach (1955) to include heat transfer to a constant temperature plate. The pressure was taken as constant throughout and solutions were obtained as a series expansion about the quasi-steady state. The first-order deviations of the velocity and temperature profiles from the quasi-steady state were computed, and these indicated that positive acceleration (of the wall in a frame of reference fixed in the fluid) results in lower heat-transfer rates if the wall is being cooled, whereas the heat transfer may or may not increase when the wall is being heated. In his treatment of the case of an external flow which fluctuates harmonically about a steady mean Ostrach confined his attention to small-amplitude fluctuations and calculated only the first-order alterations to the skin friction and heat transfer. He showed that these alterations are generally out of phase with the fluctuating velocity, but that the phase shift of the heat-transfer rate becomes very small in the incompressible limit. Moore & Ostrach (1956) calculated the time-average characteristics of the compressible boundary layer over a flat plate in nearly quasi-steady flow. They found that, in the

quasi-steady approximation, the portion of the heat transfer which is independent of Mach number is less on the average than that corresponding to steady flow at the average velocity, while that portion which depends on the Mach number is also less if the wall is being cooled.

The analyses of Lin (1957) and Kestin *et al.* (1961*b*) were concerned with harmonic oscillations superimposed on a steady stream. Lin showed that no change in the mean velocity profile occurs unless the amplitude of the fluctuating part of the main stream velocity varies along the wall. He did not consider the heat-transfer problem. Employing a power-series expansion about the steady-flow solution Kestin, Maeder & Wang were able to calculate the correction to the time-average skin-friction coefficient in the small-amplitude, low-frequency limit. They found this to be of second order in the amplitude ratio (fluctuating to steady).

Flows of this type, consisting of a steady flow with superimposed harmonic fluctuations, might be thought of as corresponding to either a plane incompressible free stream containing vorticity perpendicular to the flow plane or perhaps an acoustically disturbed compressible flow. The result that only higher-order effects on transport quantities are found in such flows might be due to the fact that the extra vorticity introduced is parallel to the vorticity of the shear flow in the boundary layer. The latter is already large, of order U/δ, where U is the mean free stream velocity and δ is the mean boundary-layer thickness. Vorticity of this magnitude is much larger than that which could be due to natural turbulence in the main flow if, of course, the scale of this turbulence is not small compared to δ.

The present investigation is concerned primarily with a basically two-dimensional steady stagnation flow. We are particularly interested in the effect of external vorticity having a certain orientation, viz. parallel to the streamlines near the boundary. Vorticity with this orientation is susceptible to amplification by stretching and thus may appear near the boundary layer with large intensity even though it is present with only small intensity at some distance from the boundary layer. We note that the stagnation-point boundary layer has a large favourable pressure gradient and Tollmien–Schlichting instability will not occur in such boundary layers. Furthermore, and more importantly, the large influence of free-steam turbulence is evidenced only in the presence of a favourable pressure gradient (see the papers by Kestin & Maeder 1957 and Kestin *et al.* 1961*b*).

The interaction between vorticity in the external flow and the two-dimensional stagnation-point boundary layer has also been considered by Stuart (1959). He obtained an exact solution of the incompressible Navier–Stokes equations when the oncoming flow contains vorticity of constant magnitude but whose direction is perpendicular to the plane of flow. Vorticity so oriented undergoes no stretching. Stuart found that the change in the shear stress due to external vorticity was proportional to the amount of (constant) external vorticity and smaller numerically at the wall than in the external stream.

The axisymmetric version of the same problem was treated by Kemp (1959). He gave an exact solution of the incompressible Navier–Stokes equations at an axisymmetric stagnation point with vorticity in the oncoming flow which varied linearly with distance from the axis. In this case the vortex lines formed closed

circles concentric to the axis of symmetry so that stretching would occur as the flow spread away from the stagnation point. By the same token such external vorticity is parallel to the vorticity due to shearing in the viscous boundary layer. Kemp calculated the changes in both shear stress and temperature gradient at the wall as functions of the ratio of vorticity in the external flow to the average vorticity in the boundary layer. He found these changes to be very nearly proportional to this ratio for values of the ratio in the interval 0 to 0·6, and that the heat transfer was affected much less than the shear shress in this range.

In the following we present a mathematical model designed to describe the effect of vorticity having the particular orientation susceptible to amplification by stretching when it is steadily transported into the stagnation-point boundary layer in a basically two-dimensional flow. Geometrically our model flow is very similar to the classical Hiemenz flow, but differs from the latter in that we permit the oncoming flow to contain distributed vorticity having the desired orientation. The vorticity is distributed periodically over the third dimension which means that the normal velocity profile far from the wall has a periodic waviness along the direction normal to the plane of the basic flow. (In the Hiemenz flow, being truly two-dimensional, the normal velocity is constant along all normals to the flow plane.) We will show that such vorticity, having a sufficiently large scale, can enter the boundary layer and significantly alter the heat transfer at the wall, even though the distortion in the velocity field due to vorticity in the distant flow is small compared to the average velocity there.

2. Mathematical model

The physical situation of interest here is that of a viscous, incompressible, steady flow in the neighbourhood of a stagnation point into which a certain amount of vorticity is steadily transported by the main stream. We are particularly interested in observing the evolution of this vorticity as it penetrates the boundary layer and the concomitant effects produced on the average value of shear stress and heat transfer at the boundary.

As the simplest mathematical model of this flow which still retains the essential three-dimensional mechanism of vorticity amplification due to stretching of vortex lines, we choose to study a basically plane stagnation-point boundary-layer flow (Hiemenz flow), but one which contains a simple type of periodic three-dimensionality capable of providing vorticity with the desired orientation. The geometry is exactly that of plane stagnation-point flow. We use a co-ordinate system with origin at the solid boundary which coincides with the (x, z)-plane. The mean flow approaches the wall from $y = +\infty$ (where it is parallel to the y-axis), divides into two equal semi-infinite streams at the wall which flow away from the stagnation point along the positive and negative x-axes. The z-axis is perpendicular to the plane of flow.

The differential equations governing the flow and energy transfer are the time-independent vorticity transport equation

$$(\mathbf{c}^*.\nabla)\,\boldsymbol{\omega}^* = (\boldsymbol{\omega}^*.\nabla)\,\mathbf{c}^* + \nu\nabla^2\boldsymbol{\omega}^*, \tag{1}$$

where

$$2\boldsymbol{\omega}^* \equiv \nabla \times \mathbf{c}^*, \tag{1a}$$

the continuity equation

$$\nabla . \mathbf{c}^* = 0, \tag{2}$$

and the time-independent energy transport equation with no dissipation

$$(\mathbf{c}^* . \nabla) T^* = (\nu/Pr) \nabla^2 T^*. \tag{3}$$

In these equations $\mathbf{c}^*$ is the velocity, $2\boldsymbol{\omega}^*$ the vorticity, T^* the temperature, ν the kinematic viscosity and Pr denotes the Prandtl number. The physical properties of the fluid are assumed constant in all that follows.

The boundary conditions to be applied at the wall are

$$\mathbf{c}^*(x, 0, z) = 0 \tag{4}$$

and

$$T^*(x, 0, z) = T_w, \tag{5}$$

while for $y \to \infty$ we require that

$$\mathbf{c}^*(x, y, z) . \mathbf{i} = u^*(x, y, z) \to a, \tag{6a}$$

$$\partial[\mathbf{c}^*(x, y, z) . \mathbf{j}]/\partial y = \partial v^*(x, y, z)/\partial y \to -a, \tag{6b}$$

$$\mathbf{c}^*(x, y, z) . \mathbf{k} = w^*(x, y, z) \to 0 \tag{6c}$$

and

$$T^*(x, y, z) \to T_\infty. \tag{7}$$

Here $\mathbf{i}$, $\mathbf{j}$, $\mathbf{k}$ are unit vectors in the x-, y-, z-directions. The reciprocal of the constant a [$= \sec^{-1}$] is the time constant of the stagnation point flow; it indicates how rapidly the tangential velocity component (u^*) outside the boundary layer increases with distance from the stagnation point measured along the boundary (x).

We next introduce the dimensionless variables

$$\left.\begin{aligned} \xi, \eta, \zeta = (a/\nu)^{\frac{1}{2}} x,\ (a/\nu)^{\frac{1}{2}} y,\ (a/\nu)^{\frac{1}{2}} z, \\ \mathbf{c} = (a\nu)^{-\frac{1}{2}} \mathbf{c}^*, \quad \boldsymbol{\omega} = \boldsymbol{\omega}^*/a, \quad T = (T_w - T^*)/(T_w - T_\infty), \end{aligned}\right\} \tag{8}$$

and, in terms of these variables, the system of equations (1) through (7) becomes

$$(\mathbf{c} . \nabla) \boldsymbol{\omega} = (\boldsymbol{\omega} . \nabla) \mathbf{c} + \nabla^2 \boldsymbol{\omega}, \tag{9}$$

$$2\boldsymbol{\omega} = \nabla \times \mathbf{c}, \tag{9a}$$

$$\nabla . \mathbf{c} = 0, \tag{10}$$

$$(\mathbf{c} . \nabla) T = (1/Pr) \nabla^2 T, \tag{11}$$

$$\mathbf{c}(\xi, 0, \zeta) = 0, \tag{12}$$

$$T(\xi, 0, \zeta) = 0, \tag{13}$$

$$\mathbf{c} . \mathbf{i} \to \xi, \quad \partial(\mathbf{c} . \mathbf{j})/\partial\eta \to -1, \quad \mathbf{c} . \mathbf{k} \to 0 \tag{14a, b, c}$$

and

$$T \to 1 \quad \text{as} \quad \eta \to \infty. \tag{15}$$

In this system the differential operators are all in terms of ξ, η and ζ.

We now investigate solutions of the type

$$\mathbf{c} . \mathbf{i} = u = U(\eta, \zeta) \xi, \tag{16a}$$

$$\mathbf{c} . \mathbf{j} = v = V(\eta, \zeta), \tag{16b}$$

$$\mathbf{c} . \mathbf{k} = w = W(\eta, \zeta), \tag{16c}$$

$$T = T(\eta, \zeta). \tag{16d}$$

Such solutions differ from the Hiemenz type in that they describe a three-dimensional flow field. The three components of vorticity in such a flow field are

$$2\boldsymbol{\omega}.\mathbf{i} = (W_\eta - V_\zeta) \equiv 2\Omega(\eta, \zeta), \tag{17a}$$

$$2\boldsymbol{\omega}.\mathbf{j} = U_\zeta \xi, \tag{17b}$$

$$2\boldsymbol{\omega}.\mathbf{k} = -U_\eta \xi. \tag{17c}$$

For convenience the subscript notation is used to represent partial differentiation with respect to ξ, η, ζ. Substitution of the equations (16) and (17) into the system of equations (9) to (11) leads to the following equations for U, V and W

$$V\Omega_\eta + W\Omega_\zeta - \Omega U = \Omega_{\eta\eta} + \Omega_{\zeta\zeta}, \tag{18}$$

$$UU_\zeta + VU_{\zeta\eta} + WU_{\zeta\zeta} - U_\zeta V_\eta + U_\eta V_\zeta = (U_{\eta\eta} + U_{\zeta\zeta})_\zeta, \tag{19}$$

$$UU_\eta + VU_{\eta\eta} + WU_{\eta\zeta} + U_\zeta W_\eta - U_\eta W_\zeta = (U_{\eta\eta} + U_{\zeta\zeta})_\eta, \tag{20}$$

$$U + V_\eta + W_\zeta = 0, \tag{21}$$

$$VT_\eta + WT_\zeta = (1/Pr)(T_{\eta\eta} + T_{\zeta\zeta}). \tag{22}$$

Equations (18), (19) and (20) represent the ξ-, η- and ζ-components respectively of the vorticity transport equation (9) and equation (21) is the continuity equation.

The boundary conditions on the functions U, V, W and T are

$$U = V = W = T = 0 \quad \text{at} \quad \eta = 0, \tag{23}$$

$$U \to 1, \quad V_\eta \to -1, \quad W \to 0, \quad T \to 1 \quad \text{as} \quad \eta \to \infty. \tag{24}$$

Upon examination of equations (19) and (20) we notice that, with the aid of equation (21), first integrals of these equations can be obtained with respect to ζ and η respectively. The two integrations lead to a single relation

$$U^2 + VU_\eta + WU_\zeta = U_{\eta\eta} + U_{\zeta\zeta} + \text{const.}$$

In order that this relation satisfy the boundary condition on U as $\eta \to \infty$ the constant of integration must be unity. Hence in the system of equations (18) through (22) we can replace (19) and (20) by

$$U^2 + VU_\eta + WU_\zeta = U_{\eta\eta} + U_{\zeta\zeta} + 1. \tag{25}$$

2.1. *Specification of mathematical form of solution*

At this point we specify the nature of the three-dimensionality which we permit the flow field to have. We seek solutions which are periodic in ζ. Let

$$U = U_0(\eta) + A \sum_{n=1}^{\infty} u_n(\eta) \cos k_n \zeta, \tag{26a}$$

$$V = V_0(\eta) + A \sum_{n=1}^{\infty} v_n(\eta) \cos k_n \zeta, \tag{26b}$$

$$W = A \sum_{n=1}^{\infty} \frac{1}{k_n} w_n(\eta) \sin k_n \zeta, \tag{26c}$$

$$T = T_0(\eta) + A \sum_{n=1}^{\infty} \theta_n(\eta) \cos k_n \zeta, \tag{26d}$$

whence if follows that

$$\left.\begin{aligned} \Omega &= A \sum_{n=1}^{\infty} \omega_n(\eta) \sin k_n \zeta, \\ 2\omega_n &= [k_n^{-1} w_n' + k_n v_n]. \end{aligned}\right\} \tag{27}$$

(Hereafter the 'prime' notation, when it appears, will signify differentiation with respect to η.) We shall refer to A simply as the 'amplitude parameter'. It is an arbitrary factor which controls the magnitude of the 'ripple' in the velocity field. At this point we do not regard it as a small parameter although the possibility of its use as such as reserved.

The quantity k_n is the dimensionless wave number of the nth harmonic component of the periodically distributed vorticity. The k_n are general positive numbers, not necessarily integers. The only restrictions imposed on the k_n are that $k_{n+1} > k_n$ for all $n \geqslant 1$ and that $k_n = nk_1$. The dimensionless fundamental wavelength, $\lambda_1 = 2\pi/k_1$, can be thought of as a measure of the size of the largest eddy present. The dimensionless wavelength or eddy size corresponding to the nth harmonic component of the vorticity is simply $\lambda_n = 2\pi/k_n$.

It should be emphasized at this point that the harmonic components u_n, v_n, etc., are *not* coefficients of Fourier cosine or sine representations of a prescribed three-dimensional disturbance. For if they were, these functions would be uniquely determined by the shape of the prescribed disturbance. In contradistinction these harmonic components are unknown functions of the co-ordinate η and, presuming solutions exist, are individually governed by the system of non-linear differential equations given above. That the basic non-linearity of these equations demands the full spectrum and not a finite number of these components is clear. Because of the non-linearity the equations governing a particular component will be coupled to all other components, and there results the exchange of energy among the harmonic components (or eddies of different size) characteristic of non-linear systems.

If we now substitute the equations (26) and (27) into equations (18), (25), (21) and (22), we obtain a system of differential equations for U_0, V_0, T_0 and the harmonic components u_n, v_n, w_n, ω_n, θ_n. First from equation (21),

$$U_0 + V_0' = 0, \tag{28}$$

and

$$u_n + v_n' + w_n = 0. \tag{29}$$

Thus if we define a function $\phi(\eta)$ such that

$$\phi(\eta) \equiv -V_0, \tag{30}$$

it follows that

$$U_0 = \phi'. \tag{31}$$

Secondly, from the definition of Ω, equation (17a),

$$2k_n \omega_n = w_n' + k_n^2 v_n. \tag{32}$$

As an alternative relation between ω_n and the velocity components of index n, combination of equations (29) and (32) yields

$$-v_n'' + k_n^2 v_n = 2k_n \omega_n + u_n'. \tag{33}$$

Upon substitution into equations (18), (25) and (22) we encounter products of pairs of the infinite sine and cosine series. With the aid of certain trigonometric identities, which for the sake of conciseness here are listed in the Appendix, we can rewrite these products as simple sine or cosine series whose coefficients are infinite sums composed of the coefficients of the original constituent series. Thus from equation (18) we arrive at

$$\omega_n'' + (\phi\omega_n)' - k_n^2\omega_n = \tfrac{1}{2}A\sum_{i=1}^{\infty}[\omega_i(v_{n-i} + v_{n+i} - v_{i-n})]' - (n/i)\,w_i(\omega_{i+n} + \omega_{i-n} - \omega_{n-i}). \quad (34)$$

Here and in all subsequent summations 'i' plays the role of a dummy index. In the expansion of the right member of this equation quantities having subscripts such as $n-i$ and $i-n$ are to be replaced by zero whenever their subscripts are zero or negative.

In like manner we obtain from equation (25) two equations

$$\phi''' + \phi\phi'' - \phi'^2 + 1 = A^2\sum_{i=1}^{\infty} u_i^2 + \tfrac{1}{2}(u_i v_i)' \quad (35)$$

and

$$u_n'' + \phi u_n' - (2\phi' + k_n^2)\,u_n - \phi'' v_n = \tfrac{1}{2}A\sum_{i=1}^{\infty} 2u_i(u_{i+n} + u_{i-n} + u_{n-i}) + [v_i(u_{i+n} + u_{i-n} + u_{n-i})]' - (n/i)\,w_i(u_{i+n} - u_{i-n} - u_{n-i}). \quad (36)$$

The first of these equations relates only those terms which are independent of ζ, whereas the second is the condition that the coefficients of the $\cos k_n\zeta$ vanish individually. Similarly, from the energy equation (22) we obtain two final equations:

$$T_0'' + Pr\phi T_0' = \tfrac{1}{2}A^2 Pr\sum_{i=1}^{\infty}(v_i\theta_i)' + u_i\theta_i, \quad (37)$$

and

$$\theta_n'' + Pr\phi\theta_n' - k_n^2\theta_n = Pr\Big\{T_0' v_n + \tfrac{1}{2}A\sum_{i=1}^{\infty}[v_i(\theta_{i+n} + \theta_{i-n} + \theta_{n-i})]' + u_i(\theta_{n+i} + \theta_{i-n} + \theta_{n-i}) - (n/i)\,w_i(\theta_{i+n} - \theta_{i-n} - \theta_{n-i})\Big\}. \quad (38)$$

Each of the equations (29), (32), (33), (34), (36) and (38) actually represents an infinity of equations while equations (35) and (37) are single equations. Hence the equations (29), (32) or (33)–(37) constitute two plus a quintuple infinity of equations for the same number of unknowns ϕ, u_n, v_n, w_n, ω_n, T_0 and θ_n, and the problem is, in principle, determinate. The equations are ordinary, generally non-linear and coupled. In principle they must be solved simultaneously for the unknowns.

2.2. *Boundary conditions*

When we substitute equations (26) into the boundary conditions (23) we obtain

$$\left.\begin{aligned} &\phi = \phi' = 0, \\ \text{and}\quad &u_n = v_n = w_n = \theta_n = 0 \quad \text{at} \quad \eta = 0. \end{aligned}\right\} \quad (39)$$

An additional condition, demanded by the continuity relation, equation (29), is

$$v_n'(0) = 0. \quad (40)$$

The boundary conditions (24) require that

$$\left.\begin{aligned} \phi' &\to 1, \quad u_n \to 0, \quad v_n' \to 0, \quad w_n \to 0 \\ \text{and} \qquad T_0 &\to 1, \quad \theta_n \to 0 \quad \text{as} \quad \eta \to \infty. \end{aligned}\right\} \tag{41}$$

Additional restrictions which we regard as implicit in the conditions (41) are that

$$\phi'', u_n', v_n'', w_n', T_0', \theta_n' \to 0 \quad \text{as} \quad \eta \to \infty, \tag{42}$$

and the same applies to all higher derivatives of these functions.

It is interesting to note that although v_n' is required to vanish far from the wall, v_n *is not*. Thus the periodic 'ripple' in the normal velocity component is allowed to have some bounded but non-zero amplitude at the edge of the boundary layer. A glance at the equations (17) for the vorticity components reveals the consequence of this: *The vorticity entering the boundary layer, i.e. being transported into it by the external flow, lies in the plane of the flow and is parallel to the wall.* The intensity of this vorticity varies sinusoidally in the direction normal to the plane of flow. This is the feature of primary importance in our model. *The vorticity transported into the stagnation-point boundary layer has the only orientation susceptible to stretching in the stagnation-point flow. In what is to follow we shall see that this incident vorticity can generate completely three-dimensional effects within the boundary layer which in turn can drastically affect the heat transfer at the wall.*

2.3. *A neutral wavelength or eddy size*

Consider the differential equation (34) governing the $\omega_n(\eta)$ for very large η. As $\eta \to \infty$, $\phi \to \eta$, $\omega_n'' \to 0$ and, by virtue of the conditions (41) and (42), the non-linear right member also becomes vanishing small. Hence we are left with a particularly simple asymptotic form for equation (34)

$$d(\eta\omega_n)/d\eta - k_n^2\omega_n = 0.$$

The solution to this equation is

$$\omega_n \to C_n \eta^{(k_n^2-1)} \quad (\eta \to \infty),$$

and we see that for $k_n^2 > 1$, ω_n grows as a positive power of η as η increases, while for $k_n^2 < 1$, ω_n decreases as a negative power of η. $k_n^2 = 1$ marks a neutral case in which ω_n has some constant non-zero magnitude at the edge of the boundary layer. The mathematical significance of this is clear: only those vorticity components for which $k_n < 1$ are compatible with the required conditions at $\eta = \infty$; those components for which $k_n > 1$ must be suppressed by putting the corresponding C_n equal to zero. Thus there is a cut-off wavelength $\lambda_0 = 2\pi$ which must be imposed on the incoming vorticity distribution. Wavelengths shorter than λ_0 (higher harmonics) cannot satisfy the governing equations of this problem and hence are not allowed. Wavelengths equal to or longer than λ_0 can enter the boundary layer.

The physical significance of the neutral wavelength or eddy size seems clear enough. As vorticity is transported toward the boundary layer it undergoes simultaneous amplification due to stretching and dissipation due to viscous action. Vorticity of scale smaller than the neutral size is dissipated more rapidly

than it is amplified, and hence decreases as the boundary layer is approached (or in other words increases as η increases away from the boundary layer). We conclude, therefore, that this smaller-scale vorticity will be dissipated into thermal energy before it can reach the boundary layer. On the other hand, vorticity of larger scale than the neutral size is amplified more rapidly than it is dissipated as it approaches the boundary layer. This larger-scale vorticity can consequently attain the boundary layer, enter it and bring about the generation of three-dimensional effects therein. The neutral scale vorticity ($k_n = 1$) experiences zero net amplification as it approaches the boundary layer and hence has an intensity which does not vary with distance until it encounters the viscous layer. It is interesting to note that in terms of the Hiemenz boundary-layer thickness δ, the neutral wavelength $\lambda_0 \approx 2{\cdot}6\delta$.

It must be emphasized that the absence of the shorter wavelengths *at the edge of the boundary layer* does not mean that these will not appear *inside the boundary layer*. On the contrary the shorter wavelengths (small eddies) will be generated through the dissipative action of viscosity on the longer wavelengths (large eddies) in the boundary layer. It will be seen from the results to follow shortly that this fundamental non-linear phenomenon is faithfully predicted by the mathematics of the model.

We attempted to achieve a solution for the particular case $k_1 = 1$. In this case λ_1, the wavelength of the first harmonic component, is equal to the neutral wavelength $\lambda_0 = 2\pi$, and λ_1 is therefore the only permissible wavelength in the entering vorticity. As a result, the asymptotic conditions to be satisfied by the spectrum of vorticity components in the computations described below are

$$\omega_1 \to \text{const.} \quad \text{and} \quad \omega_n \to 0, \quad n > 1 \quad \text{as} \quad \eta \to \infty.$$

This particular case is only one of an infinite number of possibilities contained in the domain of interest, $0 < k_n \leqslant 1$, $1 \leqslant n < \infty$, and we do not suggest that the results to follow are typical of the entire range of possibilities. The neutral-scale vorticity is representative, however, in one essential respect, namely that it persists as it is convected towards the boundary layer, albeit with no net amplification, and finally affects the flow and energy transfer within it. Since the prime objective of this analysis was to calculate the changes provoked in the boundary layer, as a means of detecting any disparity in the sensitivities of the velocity and temperature distributions, this factor was important in our choice of a numerical example. We wish to emphasize again that the nature of the vorticity content of the oncoming flow is something which is *imposed* in this theory, and it is our intention to examine additional cases in which $k_1 > 1$.

3. Approximate solutions by electronic analogue computer

In addition to being infinite in number the equations we wish to solve are coupled in very complex ways. There is, of course, no hope of achieving an exact and complete solution. However, there is a good possibility of obtaining an approximate solution which is very close to the exact one, provided the spectra of the magnitudes u_n, v_n, w_n, θ_n tail off rapidly enough with increasing n. If this be the case the system of ordinary differential equations can be conveniently

solved approximately on an electronic analogue computer and, by iteration, rapid and accurate convergence to the exact solution would be possible.

Using a PACE TR-10 Analogue Computer, we obtained first approximate solutions for ϕ, ω_1, v_1, u_1, w_1, T_0 and θ_1 for the case $k_1 = 1$ and $Pr = 0{\cdot}74$. These solutions were then used to obtain first approximations for ω_2, v_2, u_2, w_2 and θ_2. On the basis of a comparison between the second harmonics and the first we were able to conclude that, in this particular case, the next higher harmonics would be of inconsequential magnitude. Finally, we computed second approximations for ϕ and T_0. These last results gave evidence of a marked difference in the sensitivities of the mean shear stress and the mean heat transfer at the wall to the presence of the vorticity. (In this work 'mean' will always signify an average over the third dimension ζ.) For the particular numerical value assigned to the intensity of the incoming vorticity in the computations the wall shear stress was increased by 5 % while the heat transfer increased by 26 %.

We now proceed to discuss the computations in more detail and to present the graphical solutions obtained as the direct output of the computer. The discussion will not cover the details of electronic simulation such as scaling, circuitry, etc., since these are incidental matters and would consume an excessive amount of space.

A first approximation for ϕ, denoted by $\phi_{(1)}$, was obtained by solving the homogeneous version of equation (35),

$$\phi'''_{(1)} + \phi_{(1)}\phi''_{(1)} - \phi'^2_{(1)} + 1 = 0, \tag{43}$$

with the boundary conditions

$$\phi_{(1)}(0) = \phi'_{(1)}(0) = 0, \tag{44}$$

$$\phi'_{(1)} \to 1 \quad \text{as} \quad \eta \to \infty. \tag{45}$$

The function $\phi_{(1)}$, displayed in figure 1, is exactly the Hiemenz flow solution discussed in the book by Schlichting (1960). The value found for the wall shear stress, $\phi''_{(1)}(0)$ was 1·237 which differs by only 0·36 % from the corresponding value calculated by Howarth and given by Schlichting. The electronic circuit simulating equation (43) was then used to generate $\phi_{(1)}$ for use in the calculation of the first approximation for $T_{0(1)}$ which satisfied

$$T''_{0(1)} + Pr\,\phi_{(1)}T'_{0(1)} = 0, \tag{46}$$

$$T_{0(1)}(0) = 0, \quad T_{0(1)} \to 1 \quad \text{as} \quad \eta \to \infty, \tag{47}$$

with $Pr = 0{\cdot}74$. The value found for $T'_{0(1)}(0)$, which is proportional to the heat transfer at the wall, was 0·509. By comparison, the numerical result calculated by Squire and tabulated in Schlichting (1960) is 0·495 for $Pr = 0{\cdot}7$. Figure 2 shows the function $T_{0(1)}$ and its first derivative. It is interesting to note that in the pure two-dimensional flow the thickness of the thermal boundary layer in the case when $Pr = 0{\cdot}74$ is about 1·5 times that of the velocity boundary layer.

The next step in obtaining the first approximation was the simultaneous solution for $\omega_{1(1)}$ and $v_{1(1)}$. The governing approximate equations were taken to be the homogeneous version of equation (34)

$$\omega''_{1(1)} + (\phi_{(1)}\omega_{1(1)})' - \omega_{1(1)} = 0 \tag{48}$$

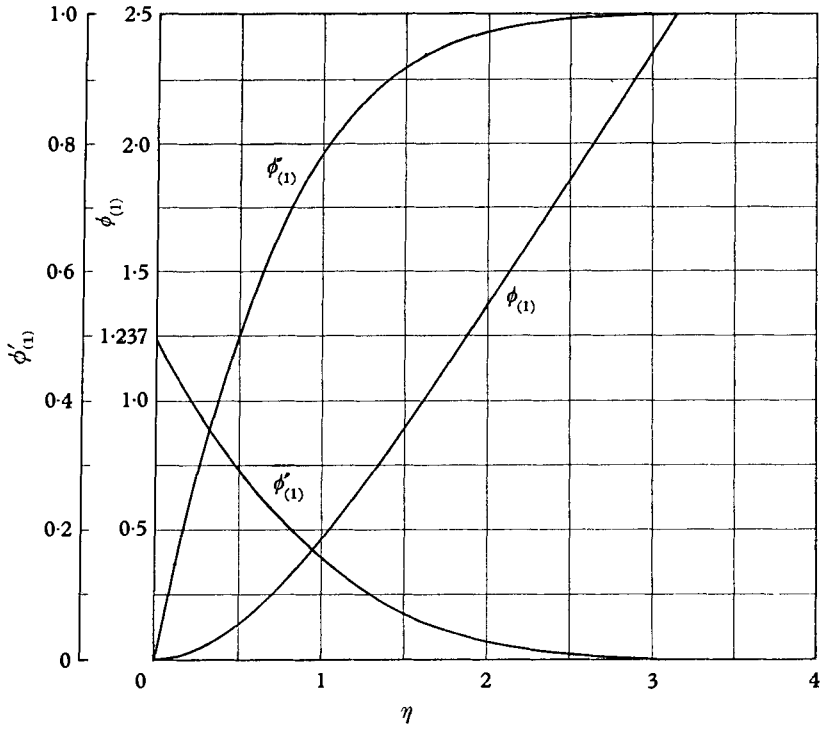

FIGURE 1. First approximation to the function ϕ; the Hiemenz solution.

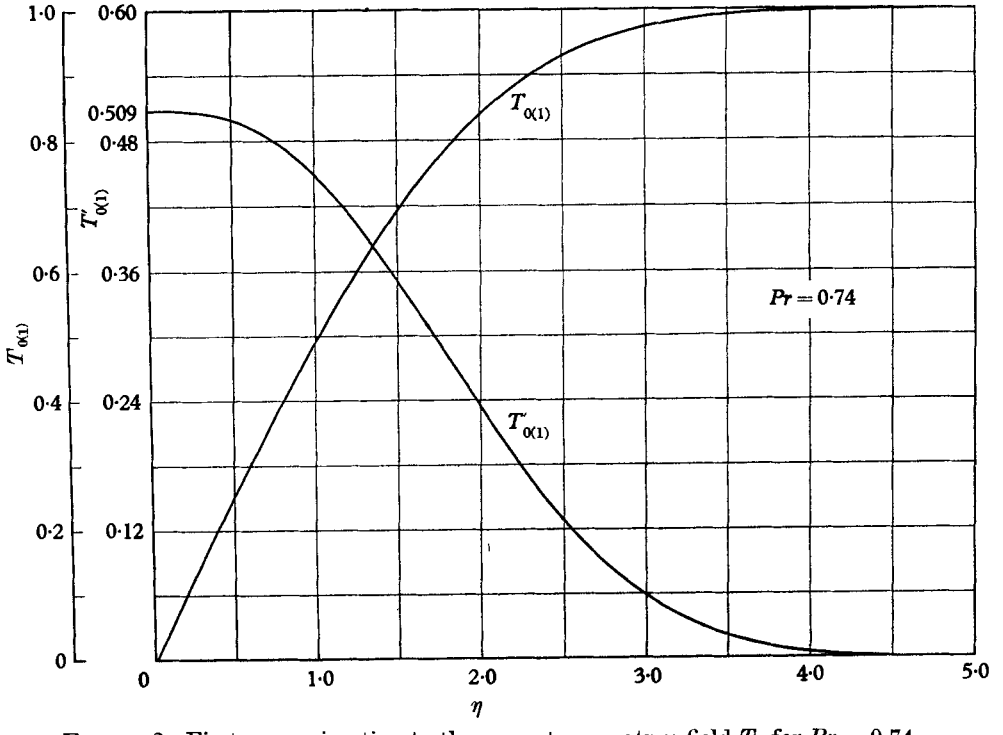

FIGURE 2. First approximation to the mean temperature field T_0 for $Pr = 0{\cdot}74$.

and equation (33) minus the u_1' term

$$v_{1(1)}'' - v_{1(1)} = -2\omega_{1(1)}. \tag{49}$$

The boundary conditions imposed were

$$v_{1(1)}(0) = v_{1(1)}'(0) = 0, \tag{50}$$

$$v_{1(1)} \to \text{const.}$$

and

$$v_{1(1)}', v_{1(1)}'', \text{ etc.} \to 0 \quad \text{as} \quad \eta \to \infty. \tag{51}$$

Although $\omega_{1(1)}$ appears to be independent of $v_{1(1)}$ in this approximate framework it is indeed coupled to $v_{1(1)}$ through the boundary conditions. There are no explicit boundary conditions on the vorticity, hence the necessity for simultaneous solution.

The u_1' term was omitted from equation (49) out of economic necessity, because at this point there was no machine capacity remaining to permit simultaneous solution for $u_{1(1)}$. (It will be recalled that, in addition to the two second-order equations for $\omega_{1(1)}$ and $v_{1(1)}$, the third-order equation for $\phi_{(1)}$ was kept on the machine as a function generator. These three equations required a total of seven integrating networks and the particular computer had only eight. The eighth was used to generate a linear time base for the plotting instrument.) We had no prior suspicion of weak coupling between u_1 and v_1 and hence no guarantee that this step was a good first approximation. Fortuitously it happened that $u_{1(1)}$ and $u_{1(1)}'$ were smaller than $v_{1(1)}$ and $\omega_{1(1)}$ by at least an order of magnitude so that, in restrospect, the assumption of a weak u_1 influence on the (ω_1, v_1)-system was quite good. This was very fortunate in view of the machine limitation mentioned above, for the necessity of solving for ω_1, v_1 and u_1 simultaneously would have complicated our work considerably. As it was, this calculation was the most difficult to perform since it entailed finding two unknown initial conditions, viz. $\omega_1(0)$ and $\omega_1'(0)$, instead of the usual one.

Since the equation governing $\omega_{1(1)}$ is both linear and homogeneous, there must be an arbitrary factor associated with the solution. Thus we see the utility of the amplitude parameter A. In solving for $\omega_{1(1)}$ we strived to adjust the initial conditions so that $v_{1(1)}$ would be of order unity at the edge of the boundary layer. (In the computation, 'order unity' was, of course, established by the capability of the machine.) According to equation (49), $2\omega_{1(1)}$ would then also be of order unity at large η. Having set $v_{1(1)} \approx 1$ and $\eta \to \infty$, we could then in subsequent calculations control the absolute size of the incoming vorticity through regulation of A. As in the case of ω_1, the relative size of the functions u_1, w_1 and θ_1 is established once the magnitude of v_1 is set. The second criterion used in the search for the unknown conditions $\omega_{1(1)}(0)$ and $\omega_{1(1)}'(0)$ was that $v_{1(1)}''$ vanish asymptotically at large η. This was the most sensitive condition on $v_{1(1)}$ that could be conveniently imposed in the course of the integration.

Our procedure consisted of first fixing one of the unknown conditions, viz. $\omega_{1(1)}(0)$. Then, while observing the function $v_{1(1)}''$ on the screen of an oscilloscope with the computer operating in a rapid repetitive mode, we adjusted the ratio of the two unknown voltages (simulating $\omega_{1(1)}(0)$ and $\omega_{1(1)}'(0)$) until the desired asymptotic behaviour was achieved. By trial and error we finally succeeded in

satisfying our dual criteria on both the magnitude and curvature of $v_{1(1)}$ at large η. Figure 3 shows the best solutions obtained for $v_{1(1)}$ and $\omega_{1(1)}$. It can be seen therein that $v''_{1(1)}$ retains a small negative value at large η. As a matter of fact this error

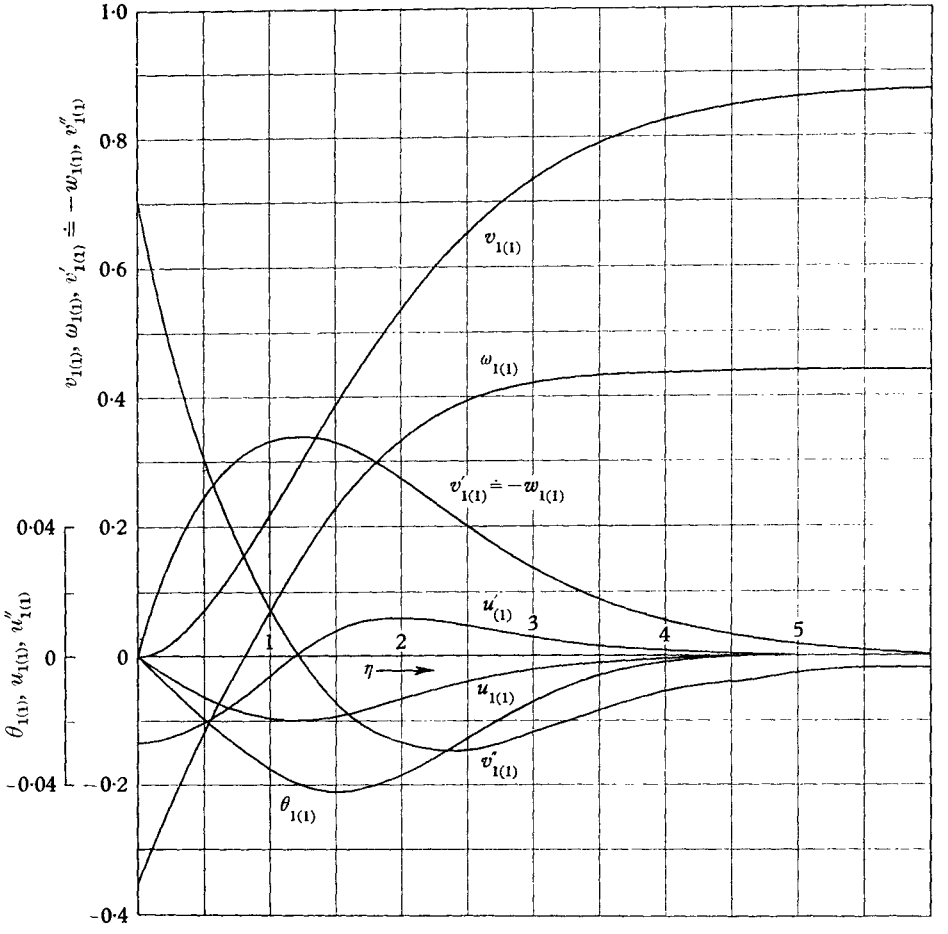

FIGURE 3. First approximations to first harmonic components of vorticity, velocity and temperature distortions $k_1 = 1$.

lies within the limits of accuracy of the machine; for it was not possible to set the potentiometers controlling the initial conditions, or any of the other coefficients, sufficiently accurately to suppress completely certain exponentially growing complementary functions at values of η as large as 5 or 6.

It is also interesting to note that $\omega_{1(1)}$ changes sign within the boundary layer. We can anticipate this behaviour by examining the complete solution of equation (49) for $v_{1(1)}$. It is

$$v_{1(1)} = e^{-\eta} \int_0^{\eta} e^{\alpha}\, \omega_{1(1)}(\alpha)\, d\alpha - e^{\eta} \int_0^{\eta} e^{-\alpha}\, \omega_{1(1)}(\alpha)\, d\alpha.$$

We see that if $v_{1(1)}$ is to be bounded as $n \to \infty$ the integral-coefficient of the positive exponential must vanish at least as rapidly as $e^{-\eta}$. Since the function

$e^{-\alpha}$ in the integrand is always positive, it follows that $\omega_{1(1)}$ must be negative for a certain interval of values of α.

The first approximation to $u_1(u_{1(1)})$ was obtained by solving equation (36) minus the infinite sum of non-linear interaction terms

$$u''_{1(1)} + \phi_{(1)} u'_{1(1)} - (2\phi'_{(1)} + 1)\, u_{1(1)} = \phi''_{(1)} v_{1(1)}, \tag{52}$$

with the boundary conditions

$$u_{1(1)}(0) = 0 \tag{53}$$

and

$$u_{1(1)} \to 0 \quad \text{as} \quad \eta \to \infty. \tag{54}$$

In this case the function $\phi''_{(1)} v_{1(1)}$ was programmed onto a variable-function diode generator which simulates any desired function from ten straight-line segments. Solution to this equation was quite straightforward otherwise. The unknown initial condition on $u'_{1(1)}(0)$ was determined so as to give the proper behaviour at large η. Figure 3 shows the function $u_{1(1)}$ and its first derivative. We see that the maximum value of $|u'_{1(1)}|$ is about 0·027 occurring at $\eta = 0$ where $|2\omega_{1(1)}| \doteq 0{\cdot}70$. Again at $\eta = 2$, $|u'_{1(1)}|$ passes through a maximum, and $|u'_{1(1)}| \doteq 0{\cdot}012$ there while $|2\omega_{1(1)}| \doteq 0{\cdot}67$ at the same location. Hence we feel justified in concluding that omission of $u'_{1(1)}$ from the equations for $v_{1(1)}$ and $\omega_{1(1)}$ could result in an error of 5 % at most in the corresponding solutions.

According to equation (29), we must have

$$w_1 = -v'_1 - u_1.$$

Examination of figure 3 reveals that the functions $v'_{1(1)}$ and $u_{1(1)}$ both attain their maximum magnitudes in the neighbourhood of $\eta = 1{\cdot}3$ wherein $|u_{1(1)}|$ is only about 6 % of $|v'_{1(1)}|$. Hence, we took

$$w_{1(1)} = -v'_{1(1)} \tag{55}$$

as a sufficiently accurate first approximation for $w_{1(1)}$.

The first approximation to θ_1 was obtained by solving

$$\theta''_{1(1)} + Pr\, \phi_{(1)} \theta'_{1(1)} - \theta_{1(1)} = Pr\, T'_{0(1)} v_{1(1)} \tag{56}$$

with

$$\theta_{1(1)}(0) = 0, \quad \theta_{1(1)} \to 0 \quad \text{as} \quad \eta \to \infty. \tag{57}$$

The solution corresponding to $Pr = 0{\cdot}74$ is also given in figure 3.

In order to compute first approximations to ω_2 and v_2 it was essential to retain in equation (34) at least an approximate representation for the infinite sum of non-linear interaction terms. The reason for this is that there are no bounded solutions to the system comprised of the homogeneous version of equation (34) and equation (33) (minus the u'_n term) for $n \geqslant 2$. That this is so can be understood by referring again to our earlier discussion of the asymptotic solution for ω_n. As the approximation to the right member of equation (34) we took

$$\tfrac{1}{2}A[(\omega_{1(1)} v_{1(1)})' + 2w_{1(1)} \omega_{1(1)}] \doteq \tfrac{1}{2}A[\omega'_{1(1)} v_{1(1)} - \omega_{1(1)} v'_{1(1)}]$$

wherein we have made use of equation (55). Hence the approximate equations used for the computation of $\omega_{2(1)}$ and $v_{2(1)}$ were

$$\omega''_{2(1)} + (\phi_{(1)} \omega_{2(1)})' - 4\omega_{2(1)} = \tfrac{1}{2}A[\omega'_{1(1)} v_{1(1)} - \omega_{1(1)} v'_{1(1)}] \tag{58}$$

and $$v''_{2(1)} - 4v_{2(1)} = -4\omega_{2(1)}, \tag{59}$$

subject to $$v_{2(1)}(0) = v'_{2(1)}(0) = 0 \tag{60}$$

and $$v'_{2(1)},\ v''_{2(1)},\ \text{etc.} \to 0 \quad \text{as} \quad \eta \to \infty. \tag{61}$$

The function $[\omega'_{1(1)} v_{1(1)} - \omega_{1(1)} v'_{1(1)}]$ was generated by means of the variable-function diode generator and the factor $\frac{1}{2}A$ was controlled by a potentiometer setting. Figure 4 shows the solutions obtained for $A = 1$. Since equations (58) and (59) are linear the numerical magnitudes shown in figure 4 may be simply scaled linearly for any other values of A; e.g. for $A = 10$ we need only multiply

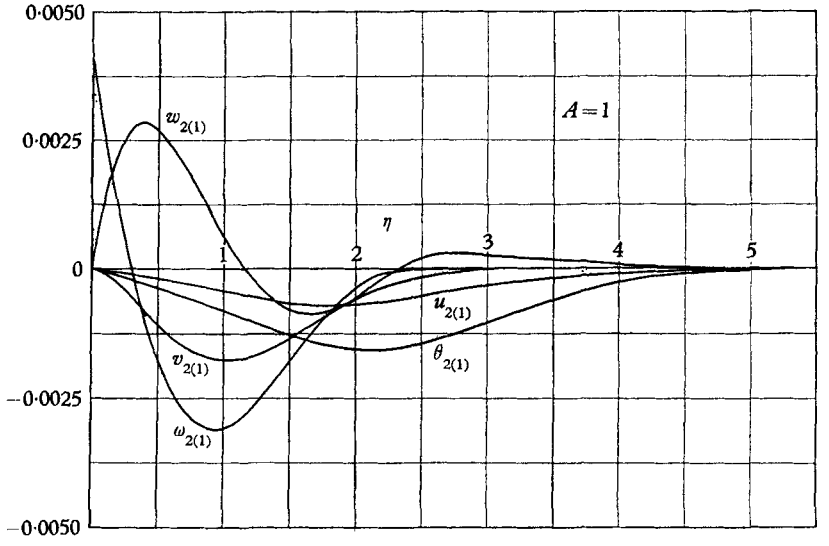

FIGURE 4. First approximation to second harmonic components of vorticity, velocity and temperature distortions $k_1 = 1$, magnitudes shown for $A = 1$.

the indicated ordinates by 10, etc. We call attention to the smallness of these magnitudes. For $A \approx 10$, $|v_{2(1)}|_{\max}$, occurring near $\eta = 1$, is less than 10% of the local value of $|v_{1(1)}|$. The maximum value of $|\omega_{2(1)}|$ occurs at the wall and is about an order of magnitude smaller than $|\omega_{1(1)}|$ at the wall when $A \approx 10$. We notice also that generation of $\omega_{2(1)}$ commences at about the edge of the classical stagnation boundary layer ($\eta \doteq 2{\cdot}4$). By comparison with figure 3, we see that within the interval $2{\cdot}4 < \eta < 0{\cdot}9$, $\omega_{2(1)}$ rises to its first maximum while $\omega_{1(1)}$ decreases steadily toward zero. This brings to mind the fundamental non-linear mechanism of spectral interaction prevalent in true turbulent flow in which large eddies give up kinetic energy to small eddies. We see also that after decreasing to zero (at different locations within the boundary layer) both $\omega_{1(1)}$ and $\omega_{2(1)}$ undergo one final amplification in the vicinity of the wall and attain relatively large magnitudes at the wall.

Also clearly evident in figures 3 and 4 is the generation of a three-dimensional velocity field. Since $w_{1(1)} \doteq -v'_{1(1)}$ and $w_{2(1)} \doteq -v'_{2(1)}$ the growth and decay of $v'_{1(1)}$ and $v'_{2(1)}$ depicted in these figures is a good illustration of how the ζ velocity component develops within the boundary layer.

In an exactly similar way solutions were obtained for $u_{2(1)}$ and $\theta_{2(1)}$ and these are also displayed in figure 4 for $A = 1$. $\theta_{2(1)}$ was calculated for $Pr = 0{\cdot}74$ only. The approximate differential equations and boundary conditions satisfied by $u_{2(1)}$ and $\theta_{2(1)}$ are the following:

$$u''_{2(1)} + \phi_{(1)} u'_{2(1)} - (2\phi'_{(1)} + 4)\, u_{2(1)} = \tfrac{1}{2}A[2v_{2(1)}\phi''_{(1)} + 2u^2_{1(1)} + v_{1(1)}u'_{1(1)} - v'_{1(1)}u_{1(1)}], \quad (62)$$

$$u_{2(1)}(0) = 0, \quad u_{2(1)} \to 0 \quad \text{as} \quad \eta \to \infty, \quad (63)$$

$$\theta''_{2(1)} + Pr\,\phi_{(1)}\theta'_{2(1)} - 4\theta_{2(1)} = \tfrac{1}{2}APr[2T'_{0(1)}v_{2(1)} + v_{1(1)}\theta'_{1(1)} - v'_{1(1)}\theta_{1(1)}], \quad (64)$$

$$\theta_{2(1)}(0) = 0, \quad \theta_{2(1)} \to 0 \quad \text{as} \quad \eta \to \infty. \quad (65)$$

In each case the function $v_{2(1)}$ is that depicted in figure 4 for $A = 1$. The right members of equations (62) and (64) were, as before, programmed on the variable-function generator which then participated directly in the computation.

3.1. *Distortion of the basic flow and heat transfer*

The final computations which we conducted were expected to reflect the influence of the three-dimensional effects on the character of the mean flow and temperature fields. We used the first approximations to the first and second harmonic quantities to calculate second approximations to ϕ and T_0, i.e. $\phi_{(2)}$ and $T_{0(2)}$. The equations solved and the associated boundary conditions are

$$\phi'''_{(2)} + \phi_{(2)}\cdot\phi''_{(2)} - \phi'^2_{(2)} + 1 = A^2\{u^2_{1(1)} + \tfrac{1}{2}(u_{1(1)}v_{1(1)})' + A^2[u^2_{2(1)} + \tfrac{1}{2}(u_{2(1)}v_{2(1)})']\}, \quad (66)$$

$$\phi_{(2)}(0) = \phi'_{(2)}(0) = 0, \quad (67)$$

$$\phi'_{(2)} \to 1 \quad \text{as} \quad \eta \to \infty, \quad (68)$$

$$T''_{0(2)} + Pr\,\phi_{(1)}T'_{0(2)} = \tfrac{1}{2}A^2Pr\{u_{1(1)}\theta_{1(1)} + (v_{1(1)}\theta_{1(1)})' + A^2[u_{2(1)}\theta_{2(1)} + (v_{2(1)}\theta_{2(1)})']\} \quad (69)$$

and

$$T_{0(2)}(0) = 0, \quad T_{0(2)} \to 1 \quad \text{as} \quad \eta \to \infty. \quad (70)$$

The use of the function $\phi_{(1)}$ in equation (69) rather than $\phi_{(2)}$, which was available for the integration of this equation, was compelled by the limited capacity of the computer. It will be seen, however, in the results to follow that $\phi_{(2)}$ and $\phi_{(1)}$ differed little. The solutions to these systems are displayed in figures 5 and 6 for one particular value of A, viz. $A = 8$. This value was used in the computation for no other reason, but that it gave rise to a clearly discernible alteration of the mean flow field as characterized by $\phi_{(2)}$. In figure 5 we can compare $\phi_{(2)}$ and $\phi_{(1)}$, the latter being identically the Hiemenz solution corresponding to $A = 0$, and we see that the mean shear stress at the wall, ϕ'', has increased from 1·237 to 1·297, a change of 4·85 %. When we make the analogous comparison in figure 6, however, we observe that the mean temperature gradient at the wall, T'_0, has increased from 0·509 ($A = 0$) to 0·639, a gain of 26·0%. Thus we discover a marked difference in the sensitivities of the velocity and temperature boundary layers of the mean flow and temperature fields to the entrance of the distributed vorticity. We recall that high sensitivity of the thermal boundary layer to small changes in the intensity of free-stream turbulence when a pressure gradient is present has been encountered in experiments.

The question is immediately raised as to the reasons for this difference in sensitivity. In an attempt to answer this we are led first to examine the right

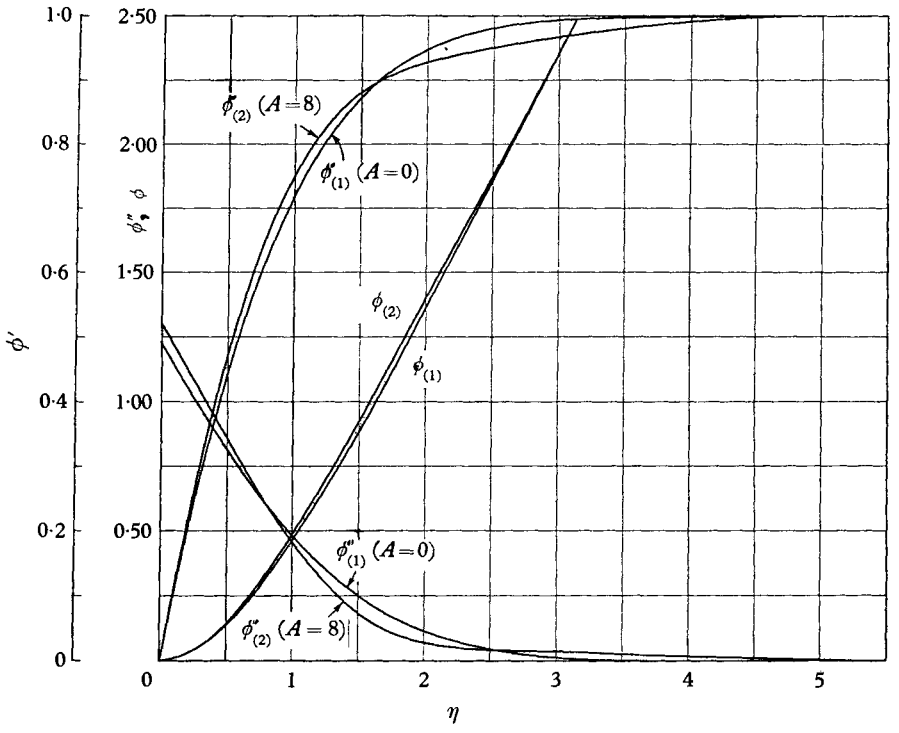

FIGURE 5. Approximate distortion of the mean flow field. Magnitude of distortion shown for $A = 8$.

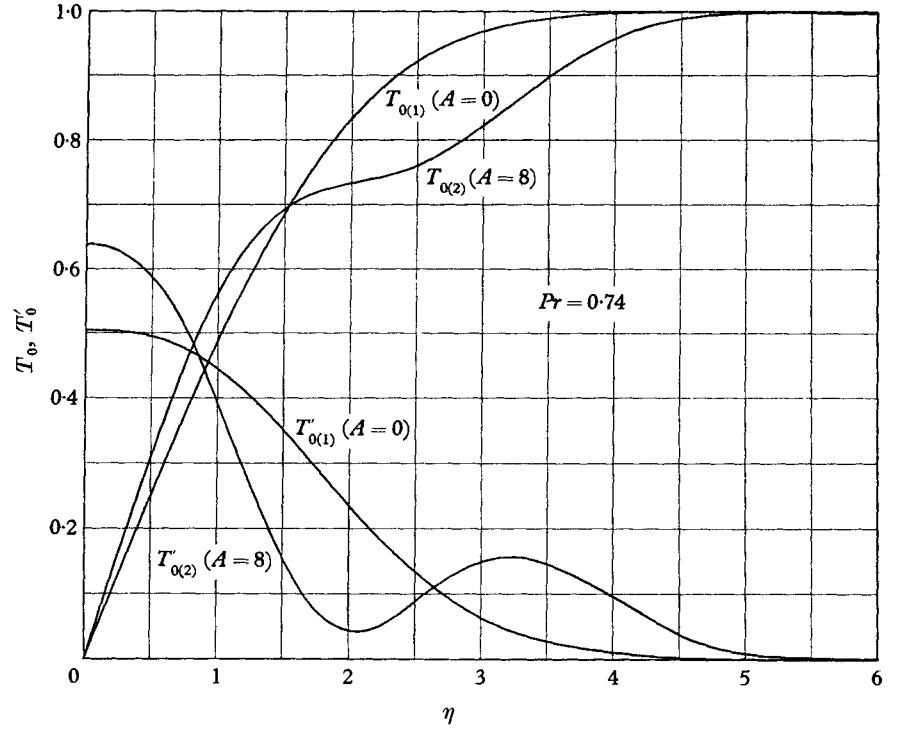

FIGURE 6. Approximate distortion of the mean temperature field magnitude of distortion shown for $A = 8$.

members of the differential equations (66) and (69) which govern the functions $\phi_{(2)}$ and $T_{0(2)}$; for it is because of these additional terms that $\phi_{(2)}$ and $T_{0(2)}$ differ from their correspondents in the undisturbed or Hiemenz flow field. Figure 7 shows the two right members in question. The right member associated with $\phi_{(2)}$ is labelled M, and the other N. We note, first, that the function N is consistently larger than M, the maximum amplitude of the latter exceeding that of the former by nearly a factor of two. Secondly, we see that the function N is clearly not a small inhomogeneity with respect to the homogeneous version of equation (69). It is, in fact, comparable in magnitude to the terms appearing in the left member of this equation. Since equation (69) is linear the difference

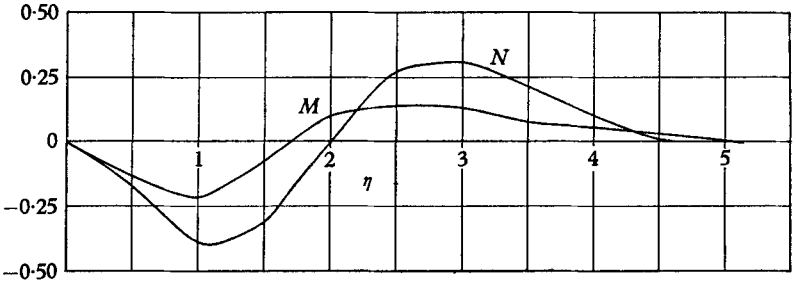

FIGURE 7. Functions representing the approximate distorting influence of added vorticity on the mean flow and temperature distributions.

between the functions $T_{0(2)}$ and $T_{0(1)}$, i.e. the distortion provoked by the vorticity, is just the particular integral. This particular integral may be visualized by comparing $T_{0(1)}$ and $T_{0(2)}$ in figure 6. We see there that the largest distortion in the mean temperature profile occurs near the edge ($\eta \doteq 2{\cdot}4$) and outside the velocity boundary layer. Just outside the velocity boundary layer the difference $T_{0(2)} - T_{0(1)}$ attains a maximum magnitude of about 0·16 or roughly 17 % of $T_{0(1)}$ locally. Within the velocity boundary layer the maximum difference is approximately 0·07, but the relative distortion ranges as high as 25 %.

We can go one step further and examine the cause for the different magnitudes possessed by the functions M and N. According to equations (66) and (69) the largest contributions to these functions come from the terms $(u_{1(1)}v_{1(1)})'$ in M and $(\theta_{1(1)}v_{1(1)})'$ in N. Then we see from figure 3 that the function $\theta_{1(1)}$, although similar in shape to $u_{1(1)}$, is consistently greater than the latter. The maximum amplitude of $\theta_{1(1)}$ is more than twice that of $u_{1(1)}$. Examination of figure 4 reveals a similar relationship between $\theta_{2(1)}$ and $u_{2(1)}$. Thus we can conclude that the more pronounced influence of the added vorticity on the mean temperature profile is due partly to the fact that the harmonic components θ_n of the periodic temperature variation are larger than the corresponding harmonic components u_n of the periodic variation in the x- or ξ-component of velocity.

We have drawn attention to the consistently smaller magnitude of the function M as one plausible reason for the relatively smaller distortion of the velocity field within the boundary layer. Nevertheless, the function M is still of substantial magnitude relative to the other terms in the differential equation for $\phi_{(2)}$. We may, for instance, regard the function M as an additional effective pressure

gradient due to three-dimensional effects. The pressure gradient in the Hiemenz flow is represented by the term unity, so that our boundary-layer equation differs from Hiemenz' by an additional η-dependent pressure gradient. Although this additional pressure gradient attains a magnitude as large as 20 % of the constant part, the resulting function $\phi_{(2)}$ differs from the Hiemenz function $\phi_{(1)}$ by 5 % at most. It is believed that the complete explanation for this small

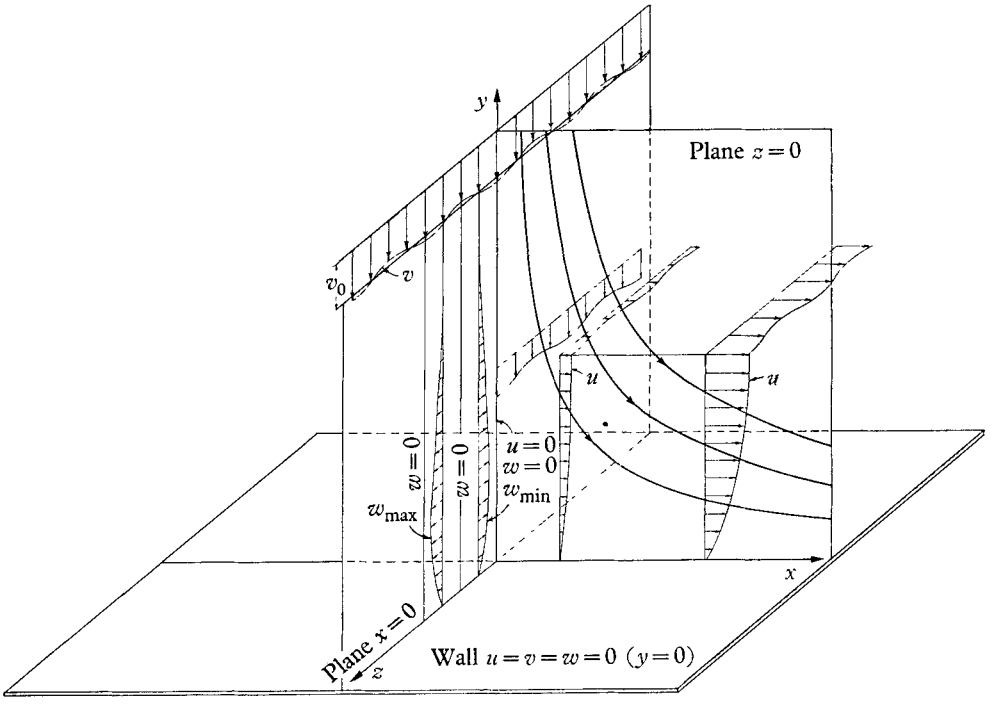

FIGURE 8. Qualitative variation of velocity component.

distortion lies in the non-linear character of the subject differential equation and in the highly restrictive nature of the boundary conditions at the wall. In addition to the explicit conditions on the function $\phi_{(2)}$ and its first derivative at $\eta = 0$, the fact that $M(0) = 0$ effectively requires that $\phi'''_{(2)}(0) = -1$. Thus the lowest derivatives which can vary at the wall are the second and the fourth. Under these circumstances it becomes obvious that the two functions $\phi_{(1)}$ and $\phi_{(2)}$ can differ very little for small values of η, i.e. near the wall.

In figure 8 we attempt to depict in a qualitative way the three-dimensional velocity field in the neighbourhood of the stagnation point. Figure 9 shows the variation of the ratio $r = A\,|v_{1(1)}|/|V_{0(1)}|$ with normal distance from the stagnation point. The numerical magnitudes indicated on the graph are calculated for $A = 8$. For large η the ratio decreases very nearly as η^{-1}. We see from this last graph that the magnitude of the disturbance used in the calculation of the distortions displayed in figures 5 and 6 corresponds roughly to a 10 % ripple in the normal velocity profile at a distance $\eta \doteq 70$, or about 30 boundary-layer widths from the wall.

3.2. *Preliminary results for the case* $Pr = 7$

In so far as they bear upon the phenomenon of heat transfer in the stagnation-point boundary layer the numerical results presented above can be regarded as representative for most common gases. It is of interest to know whether the sensitivity of the thermal boundary layer would be significantly different in a fluid with Prandtl number substantially greater than unity. We made some preliminary computations for the case $Pr = 7{\cdot}0$, corresponding to water at about 60 °F, and the results indicated a markedly greater sensitivity of the heat transfer

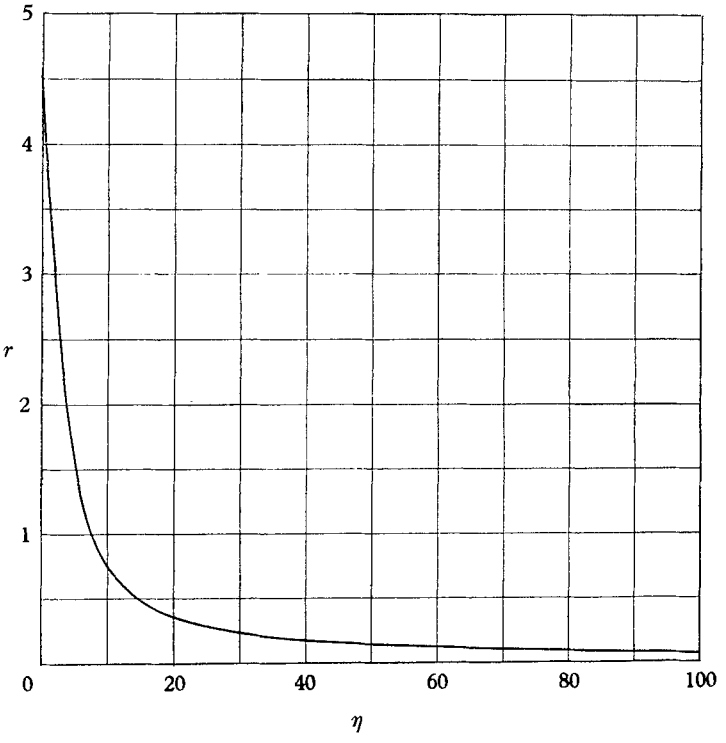

FIGURE 9. Approximate ratio of ripple amplitude to mean velocity for the normal velocity component $r = A\,|v_{1(1)}|/|V_{0(1)}|$ plotted for $A = 8$.

than that calculated for $Pr = 0{\cdot}74$. To be specific we found that neutral-scale vorticity characterized by the same intensity value, $A = 8$, and thus capable of effecting the same 5 % increase in the mean wall shear stress, provoked a 70 % increase in the mean temperature gradient at the wall. Intuitively we expect this effect of the Prandtl number because it occurs as a coefficient of the right member of the equation for $T_{0(2)}$, and hence magnifies or attenuates any given distorting influence according to whether it is greater or less than unity. Actually the influence of the Prandtl number on the particular integral is more involved than this since it occurs in the left member of the differential equation as well and since the functions θ_n also depend on Prandtl number; preliminary computations for $\theta_{1(1)}$ corresponding to $Pr = 7{\cdot}0$ show this function to be generally greater in magnitude and in slope than $\theta_{1(1)}$ corresponding to $Pr = 0{\cdot}74$.

4. Concluding remarks

We have presented a mathematical model for the interaction of vorticity in the oncoming flow with the two-dimensional stagnation-point boundary layer. The essential feature of the model is that the vorticity added to the oncoming flow is unidirectional and oriented so that the vortex lines are susceptible to stretching. An incompressible, constant-property fluid was assumed throughout. Employing iterative techniques and an electronic analogue computer we have obtained an approximate solution to the full Navier–Stokes equations as they apply to this model. The heat-transfer problem was treated simultaneously. This approximate solution indicates that:

(1) Amplification by stretching of vorticity of sufficiently large scale can occur. As a consequence, such vorticity, if present in the oncoming flow with a small intensity, can appear near the boundary layer with an amplified intensity.

(2) There is a neutral scale for vorticity, about 2·6 times the Hiemenz boundary-layer thickness, which is transported by the stagnation flow to the boundary layer with no net amplification or dissipation. Vorticity of smaller scale is dissipated before it reaches the boundary layer while the larger-scale vorticity undergoes net amplification until it reaches the boundary layer.

(3) This vorticity can enter the boundary layer and induce substantial three-dimensional effects therein. The thermal boundary layer is apparently much more sensitive to the induced effects than the velocity boundary layer. According to our computations a certain amount of distributed vorticity in the oncoming flow causes the shear stress at the wall to increase by 5 % while the heat transfer there is augmented by 26 % in a fluid with Prandtl number equal to 0·74. The sensitivity of the thermal boundary layer increases with Prandtl number.

The computations reported in this work were performed for the particular case of an oncoming flow which contains only the neutral-scale vorticity. Vorticity of smaller scale was found to be generated within the boundary layer by non-linear processes. In the opinion of the authors, it would be instructive to carry out the computations for an oncoming stream which contains vorticity of scale larger than the neutral. Such a vorticity content would correspond more closely to the physical situation in a true turbulent stream.

The research described in this paper is part of the research program of heat transfer in unsteady flows of the Aeronautical Research Laboratories, Office of Aerospace Research of the U.S. Air Force whose support is gratefully acknowledged.

Appendix. Trigonometric identities

We start with

$$\left(\sum_{m=1}^{\infty} a_m \sin k_m \alpha\right)\left(\sum_{\nu=1}^{\infty} b_\nu \sin k_\nu \alpha\right) = \sum_{m=1}^{\infty} a_m \sum_{\nu=1}^{\infty} b_\nu \sin k_m \alpha \sin k_\nu \alpha$$

$$= \frac{1}{2}\sum_{m=1}^{\infty} a_m \left\{\sum_{\nu=1}^{\infty} b_\nu \cos (k_m - k_\nu)\alpha - \sum_{\nu=1}^{\infty} b_\nu \cos (k_m + k_\nu)\alpha\right\}. \quad \text{(A 1)}$$

Since $k_m = mk_1$ and $k_\nu = \nu k_1$, $k_m - k_\nu = (m-\nu)k_1 = k_{m-\nu}$, etc. Thus we can write the right member of equation (A 1) in the form

$$\frac{1}{2}\sum_{m=1}^{\infty} a_m\left\{\sum_{\nu=1}^{\infty} b_\nu \cos k_{m-\nu}\alpha - \sum_{\nu=1}^{\infty} b_\nu \cos k_{m+\nu}\alpha\right\}. \tag{A 2}$$

By expanding a few terms of each summation within braces and making suitable changes in the dummy summation index, we see that the first sum within the braces can be rewritten as

$$\begin{aligned}\sum_{\nu=1}^{\infty} b_\nu \cos k_{m-\nu}\alpha &= \sum_{p=1}^{m-1} b_p \cos k_{m-p}\alpha + b_m + \sum_{p=1}^{\infty} b_{m+p} \cos k_p\alpha \\ &= \sum_{p=1}^{m-1} b_{m-p} \cos k_p\alpha + b_m + \sum_{p=1}^{\infty} b_{m+p} \cos k_p\alpha,\end{aligned} \tag{A 3}$$

wherein use has been made of the fact that

$$\cos k_{m-\nu}\alpha = \cos k_{\nu-m}\alpha.$$

The second sum within the braces of equation (A 2) can also be re-expressed as

$$\sum_{\nu=1}^{\infty} b_\nu \cos k_{m+\nu}\alpha = \sum_{p=m+1}^{\infty} b_{p-m} \cos k_p\alpha. \tag{A 4}$$

We can then combine equations (A 3) and (A 4) to obtain

$$\sum_{\nu=1}^{\infty} b_\nu \cos k_{m-\nu}\alpha - \sum_{\nu=1}^{\infty} b_\nu \cos k_{m+\nu}\alpha = b_m + \sum_{p=1}^{\infty} (b_{m-p} + b_{m+p} - b_{p-m}) \cos k_p\alpha. \tag{A 5}$$

In equation (A 5) a negative or zero subscript on a coefficient b_ν means that we must replace that coefficient by zero since b_ν is not defined for $\nu \leqslant 0$. Finally, we arrive at the identity of desired form

$$\begin{aligned}&\left(\sum_{m=1}^{\infty} a_m \sin k_m\alpha\right)\left(\sum_{\nu=1}^{\infty} b_\nu \sin k_\nu\alpha\right) \\ &\qquad = \frac{1}{2}\sum_{m=1}^{\infty} a_m\left\{b_m + \sum_{p=1}^{\infty} (b_{m-p} + b_{m+p} - b_{p-m}) \cos k_p\alpha\right\}.\end{aligned} \tag{A 6}$$

In an entirely similar manner we derive two additional identities

$$\begin{aligned}&\left(\sum_{m=1}^{\infty} a_m \cos k_m\alpha\right)\left(\sum_{\nu=1}^{\infty} b_\nu \cos k_\nu\alpha\right) \\ &\qquad = \frac{1}{2}\sum_{m=1}^{\infty} a_m\left\{b_m + \sum_{p=1}^{\infty} (b_{m+p} + b_{m-p} + b_{p-m}) \cos k_p\alpha\right\},\end{aligned} \tag{A 7}$$

and

$$\begin{aligned}&\left(\sum_{m=1}^{\infty} a_m \sin k_m\alpha\right)\left(\sum_{\nu=1}^{\infty} b_\nu \cos k_\nu\alpha\right) \\ &\qquad = \frac{1}{2}\sum_{m=1}^{\infty} a_m\left\{\sum_{p=1}^{\infty} (b_{p-m} + b_{p+m} - b_{m-p}) \sin k_p\alpha\right\}.\end{aligned} \tag{A 8}$$

REFERENCES

GEIDT, W. H. 1951 Effect of turbulence level of incident air stream on local heat transfer and skin friction on a cylinder. *J. Aero. Sci.* **18**, 725.

KEMP, N. H. 1959 Vorticity interaction at an axisymmetric stagnation point in a viscous, incompressible fluid. *J. Aero/Space Sci.* **26**, 543.

KESTIN, J. & MAEDER, P. F. 1957 Influence of turbulence on the transfer of heat from cylinders. *NACA TN* 4018.

KESTIN, J., MAEDER, P. F. & SOGIN, H. H. 1961 The influence of turbulence on the transfer of heat to cylinders near the stagnation point. *Z. angew. Math. Phys.* **12**, 115–32.

KESTIN, J., MAEDER, P. F. & WANG, H. E. 1961*a* Influence of turbulence on the transfer of heat from plates with and without a pressure gradient. *Int. J. Heat Mass Transf.* **3**, 133–54.

KESTIN, J., MAEDER, P. F. & WANG, H. E. 1961*b* On boundary layers associated with oscillating streams. *Appl. Sci. Res.* A, **10**, 1.

LIGHTHILL, M. J. 1954 The response of laminar skin friction and heat transfer to fluctuations in the stream velocity. *Proc. Roy. Soc.* A, **224**, 1.

LIN, C. C. 1957 Motion of the boundary layer with a rapidly oscillating external flow. *Proc. 9th Int. Congr. Appl. Mech.* **4**, 155.

MOORE, F. K. 1951 Unsteady laminar boundary layer flow. *NACA TN* 2471.

MOORE, F. K. & OSTRACH, S. 1956 Average properties of compressible laminar boundary layer with unsteady flight velocity. *NACA TN* 3886.

OSTRACH, S. 1955 Compressible laminar boundary layer and heat transfer for unsteady motions of a flat plate. *NACA TN* 3569.

SATO, K. & SAGE, B. H. 1958 Thermal transfer in turbulent gas streams: Effect of turbulence on macroscopic transport from spheres. *Trans. ASME*, **80**, 1380.

SCHLICHTING, H. 1932 Berechnung ebener periodischer Grenzschichtströmungen. *Phys. Z.* **33**, 327.

SCHLICHTING, H. 1960 *Boundary Layer Theory* (transl. J. Kestin). New York: McGraw-Hill.

SHORT, W. H., BROWN, R. A. S. & SAGE, B. H. 1960 Thermal transfer in turbulent gas streams. Effect of turbulence on local transport from spheres. *J. Appl. Mech.* **27**, 393.

STUART, J. T. 1959 The viscous flow near a stagnation point when the external flow has uniform vorticity. *J. Aero/Space Sci.* **26**, 124.